Fault identification of rotating electric machines using comparative analysis methods

Conference Paper · September 2011

DOI: 10.1109/ACEMP.2011.6490610

5 authors, including:

Horia Balan
Universitatea Tehnica Cluj-Napoca

Buzdugan Mircea Ion
Universitatea Tehnica Cluj-Napoca

Petros Karaisas
University of West Attica

Fault Identification on Electrical Machines Based on Experimental Analysis

Balan H. 1[1], Buzdugan M. I. 2[2], Karaisas P. 3[3]

[1] Technical University of Cluj Napoca, 28, Memorandumului Street, Cluj Napoca, Romania

Email of Author 1: horia.balan@eps.utcluj.ro

[2] Technical University of Cluj Napoca, 28, Memorandumului Street, Cluj Napoca, Romania

Email of Author 2: mircea.buzdugan@insta.utcluj.ro

[3] T. E. I. of Piraeus, 250th Petrou Ralli & Thivon Street, 12244 Egaleo Athens, Greece

Email of Author 3: karaisas@teipir.gr

Abstract

The paper reviews the main faults identification of electric machines based on amplitude versus time and amplitude vs. frequency vibration analysis. The aim of the paper is to introduce a new method in determining rotor faults based on stator vibration. The analysis method uses a multi-channel vibration analyzer provided with three accelerometers, set in a plane perpendicular to the stator axis. The method is suitable for determining rotor faults generated by the stator vibrations, other than those due to current harmonic components or supply voltage unbalance. The SvanPC software allowed the determination of the characteristics regarding velocity vibration vs. time and vs. frequency. Their interpretation permitted to determine the fault points on electrical machines in two industrial applications.

Keywords: Motor Vibrations Signature Analysis-MVSA, Motor Current Signature Analysis-MCSA, Experimental Analysis-EVA.

1 Introduction

Monitoring and diagnosis of electrical machines significantly reduce maintenance costs and unexpected fault hazard, allowing an early detection of their improper operation.

Incorrect operating conditions [1], [2], may lead to faults on the main parts of an electrical machine: stator, rotor, slide bearings and other types of faults.

Almost 38% of the faults are located in the stator [3]. Stator windings are placed in slots and a lower insulation resistance leads to overloads or short-circuit currents. Faulty currents determine the stator overheating, leading to unbalanced magnetic fields in the air gap and unacceptable magnitudes of the vibration of the machine.

On the other hand, rotor faults [4], [5], [6], represent approximately 10% of the total amount of faults (usually faulty rotor bars which lead to local overheating and vibration of the rotor [7]).

Most electrical machines are provided with slide bearings (ball bearings) [8], their faults representing 40% of the total amount of faults, determining undesired rotational speed changes [9] and bearing eccentricities [10].

Other types of faults (12% of the total amount of faults) are represented by rotor eccentricities with respect to the stator determining air gap non-uniformities. Changes in the air gap modify the magnetic field distribution and consequently a magnetic force on the minimum air gap direction, leading to mechanical vibrations.

Monitoring and diagnosis techniques of the electric machines operation are divided in passive and active techniques. The passive ones consist in measurements which do not affect the normal operation of the machines, while the active ones use control elements (e.g. inverters), modifying their operating conditions.

There are different monitoring techniques, depending on the signals involved:

- electrical signals monitoring (currents or voltages) or of the angular difference between the rotor and the armature, is suitable in detecting and evaluating electric faults [11].
- magnetic values monitoring, is based on measurements of the induced voltage in the rotating coils placed in the armature slots or outsides them, similar to Rogowski coils [12].
- vibrations monitoring, uses accelerometers measuring the velocity and the acceleration due to mechanical unbalances; this method is used in mechanical fault diagnosis, this type of faults being difficult to detect using electrical signals measurement.
- temperature monitoring can be performed using direct measurements or analysis performed on different models, because modifications in the temperature's field derive from electrical or mechanical faults [4], [13].
- acoustic emission monitoring, is based on the acoustic noise emitted by electrical machines in operation [14]. This type of monitoring is quite difficult to be used in industrial environment, due to the ambient noise which alters the measuring process.

The difficult part comes after monitoring the process, consisting in the analysis of the monitored data. The most known techniques on this issue are the time domain analysis [15] [16] and in the frequency domain analysis [17].

Lately several new techniques in locating the fault were developed:

- use of wavelet transform technique [18], [19]
- analysis of the dynamic time warping technique[20]

- vector techniques [21].

2 Motor Vibrations Signature Analysis-MVSA.

Analysis performed in amplitude vs. time and amplitude vs. frequency domains are the basis of electric machines vibration signature. The limit values in electric machines standards set vibration velocity as a compulsory value to be measured. The diagrams representing vibration velocity versus frequency permit to determine the RMS value of the vibration damping v_{eff} , according to the following procedure.

$$m \cdot \frac{d^2x}{dt^2} + c \cdot \frac{dx}{dt} + k \cdot x = F(t) \tag{1}$$

where:
- *m*: mass of the system;
- *k*: dynamic stiffness coefficient
- *c*: dynamic viscosity coefficient
- *x(t):* vibration of vertical amplitude
- *F*(*t*): vibration excitation force

Neglecting the damping of the system, the instantaneous amplitude of vibration $x(t)$ becomes:

$$x(t) = \frac{F_0}{k(1-r^2)} \cdot \sin \omega t \tag{2}$$

where:

$$r = \frac{\omega}{\omega_n} \text{ and } \omega_n = \sqrt{\frac{k}{m}} \tag{3}$$

If the system presents natural oscillations (oscillates at the resonance frequency), the vibration amplitude is high even for a low excitation force. The frequency value is:

$$f_n = \frac{\omega_n}{2 \cdot \pi} = \frac{2}{2 \cdot \pi}\sqrt{\frac{k}{m}} \tag{4}$$

and the corresponding speed of the critical frequency:

$$RPM_{cr} = 60 \cdot f_n = \frac{60}{2 \cdot \pi} \cdot \sqrt{\frac{k}{m}} \tag{5}$$

The force transmitted to the floor is:

$$F_T = k \cdot x \tag{6}$$

In the case of harmonic vibrations, with the instantaneous value of the vibration velocity:

$$v_i = \hat{v} \cdot \cos \omega_1 t \tag{7}$$

or of complex vibrations (i.e. a superposition of harmonic vibrations), vibration's intensity is defined as the root mean square value (RMS value) of the oscillation velocity.

The RMS value is calculated from the time diagrams of the vibration's velocity using equation (8):

$$v_{eff} = \sqrt{\frac{1}{T} \int_0^T v^2(t) \cdot dt} \tag{8}$$

Acceleration, speed and displacement amplitudes $(\hat{a}_j; \hat{v}_j; \hat{s}_j;\ j = 1, 2..., n)$ can be derived as functions of the rotating speed $(\omega_1, \omega_2, ...\omega_n)$. The RMS value was calculated according to ISO 10816 Standard, using equation (9):

$$\begin{aligned} v_{eff} &= \sqrt{\frac{1}{2} \cdot \left[\left(\frac{\hat{a}_1}{\omega_1} \right)^2 + \left(\frac{\hat{a}_2}{\omega_2} \right)^2 + \ldots + \left(\frac{\hat{a}_n}{\omega_n} \right)^2 \right]} = \\ &\sqrt{\frac{1}{2} \left(\hat{s}_1^2 \cdot \omega_1^2 + \hat{s}_2^2 \cdot \omega_2^2 + \ldots + \hat{s}_n^2 \cdot \omega_n^2 \right)} = \\ &\sqrt{\frac{1}{2} \cdot \left(\hat{v}_1^2 + \hat{v}_2^2 + \ldots + \hat{v}_n^2 \right)} \end{aligned} \tag{9}$$

If there are no vibration components with slightly close frequencies which could generate a beat phenomenon, the RMS value of the vibration velocity can be calculated as:

$$v_{eff} = \sqrt{\frac{1}{2} \cdot \left(\hat{v}_{\max}^2 + \hat{v}_{\min}^2 \right)} \tag{10}$$

where:
$\hat{v}_{\max}$: the peak value at the maximum value of the envelope curve
$\hat{v}_{\min}$: the peak value at the minimum value of the envelope curve

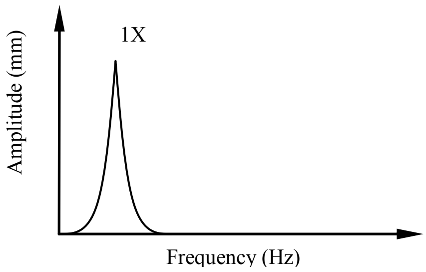

a-dynamic unbalance

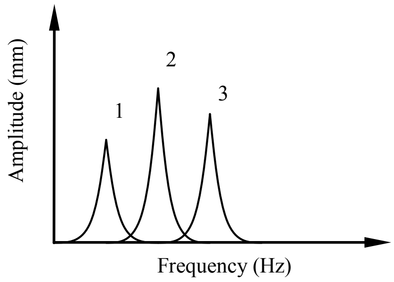

b-rotor and stator misalignment

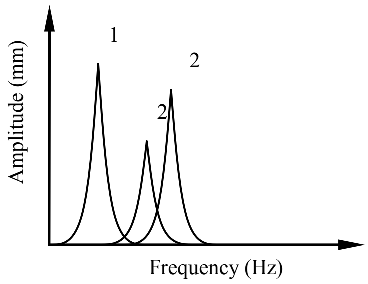

c-stator eccentricity

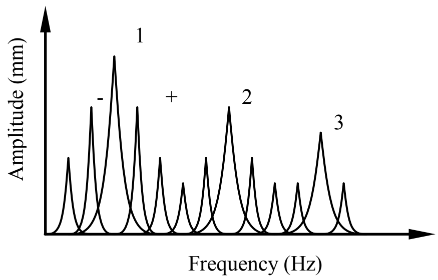

d-rotor eccentricity

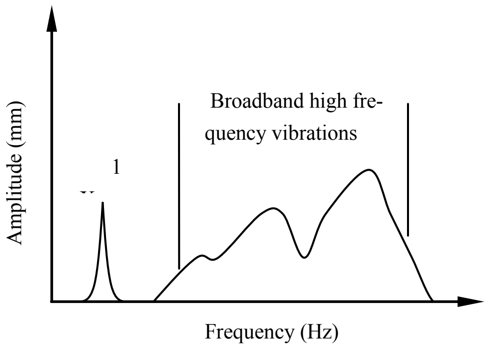

e-faulty bearings

Fig. 1 The fault identification on the electrical machine.

If the RMS value is measured using a measuring device, the RMS velocity will be approximately:

$$v_{eff} = \sqrt{\frac{1}{2} \cdot \left(R_{\max}^2 + R_{\min}^2 \right)} \tag{11}$$

where:

$R_{\max}$: the maximum value indicated by the measuring device

$R_{\min}$: the minimum value indicated by the measuring device

As the RMS value calculated according to (11) is not an accurate one, it is advisable to use this method only for very low beat frequencies.

The above analysis allows setting vibration's velocity in the limits imposed in the standards. If the limits are exceeded, analysis of the vibration velocity vs. frequency permits the fault identification on the electrical machine [25]:

- in the case of dynamic unbalance (Fig. 1a), a 1X harmonic component, different from the rotational speed occurs;
- rotor and stator misalignment issue (Fig. 1b) determines in the frequency spectrum three components, i.e. 1X, 2X and 3X;
- improper connections, insulation faults between laminates and phase unbalance (Fig. 1c) determine the frequency components 1X, 2X and 2FL, the latest having the same frequency as the supply voltage;
- rotor eccentricity (Fig. 1d), caused by faults on rotor bars, commutator or bearings, determine the frequency components 1X, 2X, 3X and –PPF and +PPF (due to adjacent poles);
- bearing faults (Fig. 1e) determine a continuous high frequency spectrum, beyond the frequency 1X.

3 Motor Current Signature Analysis-MCSA.

The purpose of this approach is the fault detection on electrical machines using vibrations' signature analysis as a diagnosis and maintenance tool, so electrical values (supply voltage unbalance or current's harmonics) are not taken into account. The point is to locate non-electrical faults, i.e. mechanical faults, their location being established after measuring the current signature determined by vibrations.

The stator current amplitude-frequency signature highlights electrical and mechanical faults:

- Current unbalance (Fig. 2) is determined by stator infrastructure faults: insulation damage of the laminated sheets or high contact resistance and overloads or short-circuits.

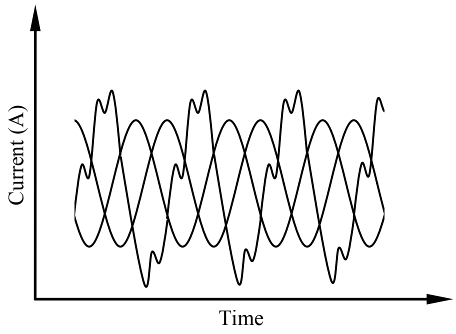

Fig. 2 Stator current asymmetry

- Vibrations due to asymmetries can be highlighted using an asymmetric supply system of the electric motor provided by a programmable source (15003iX-CTS, California Instruments). The RMS voltages in the supply lines are: line a- 220 V, line b- 165 V and line c- 110 V. The vibration amplitude vs. time waveforms are depicted in Fig. 3, the vibration measurements being performed using three transducers coplanar mounted on the stator, displaced by 120°.
- Vibrations due to current harmonics can be generated using the same programmable source. Harmonic components determined by the motor or by the source (Fig. 3) cause vibrations. As the ratio between the harmonic components and the fundamental component becomes more significant, it generates a large spectrum of vibrations, depicted by the amplitude versus frequency characteristics (Fig. 4).

Fig. 3 Vibrations amplitudes of the asymmetric supplied stator

- Rotor electrical faults are represented by the breaking of bars and/or slip rings and higher contact resistance. The frequency spectrum of the current presents harmonic components around the fundamental frequency. The frequency of the harmonic components can be calculated using equation (12) [5]:

$$f_b = \left(\frac{k}{p \cdot (1-s)} \pm s \right) \cdot f_1; \frac{k}{p} = 1,3,5... \tag{12}$$

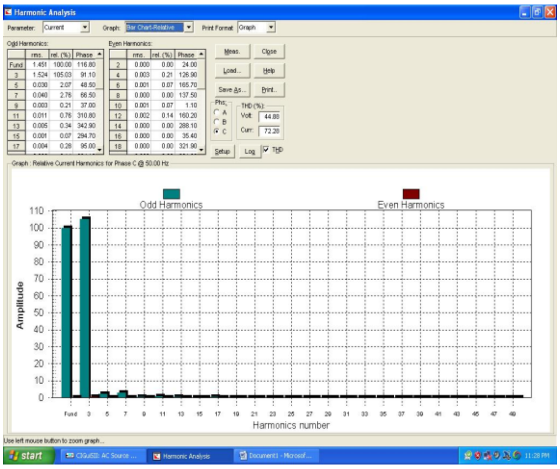

Fig. 4 Motor supplied at the line frequency and the third harmonic component

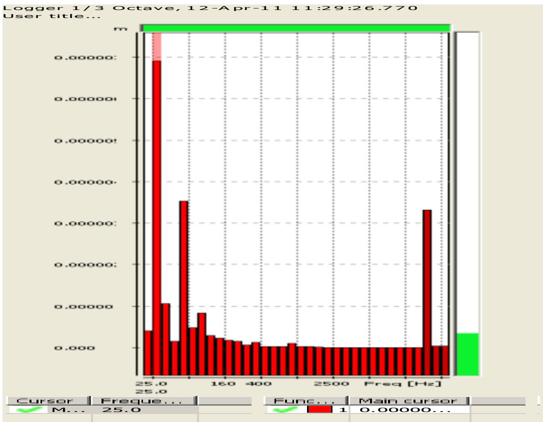

Fig. 5 Vibration spectrum of harmonic current

where f_1 is the frequency of the power supply, *s* the motor slip and *p* the pole pairs number. The adjacent poles are determined from the ratio *k*/*p* and correspond to the oscillation frequencies of the rotor [7]. The spectrum of the current (Fig. 6 a) presents frequency side bands modulated around the oscillating frequency of the rotor (1X).

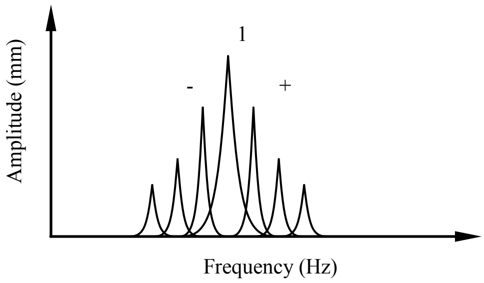

a-frequency spectrum of the current for electrical faults in rotor

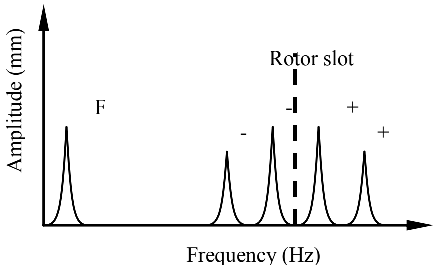

b-current frequency spectrum in case of stator eccentricities

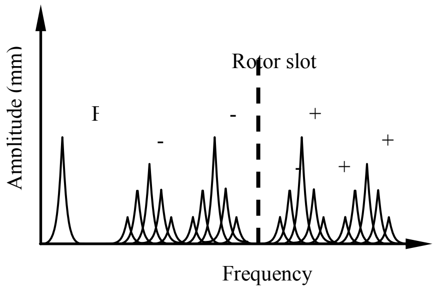

c-current frequency spectrum in case of rotor eccentricities

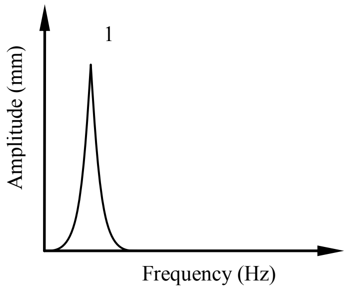

d-current frequency spectrum in case of misalignment

Fig. 6 Current frequency spectrum

- Eccentricities with respect to the rotation axis are present both in the case of the rotor and stator. The spectrum of the current differs, depending on the fault location: in stator (static eccentricity) or in rotor (dynamic eccentricity).

Static eccentricity is determined by the modification of the stator axis with respect to the rotation axis and occurs when the ball bearing lager is oval. This type of fault determines in the spectrum of the current distortions whose frequencies are calculated using equation (13):

$$f_{static} = \left((k \cdot n) \cdot \left(\frac{1-s}{p} \right) \pm v \right) \cdot f_1 \tag{13}$$

where k is a positive constant, n the slots number and v the harmonic order.

Static eccentricity of the stator leads to the premature aging of the slide bearings and balls damage.

Current spectrum analysis highlights the presence of the side bands $\pm$ FL and $\pm$ 3 FL, around the rotation frequency of the rotor slots (Fig. 6 b).

Dynamic eccentricities [15] occur when the rotor axis does not correspond with the normal rotation axis and are present in the case of bent rotors or in the presence of mechanical resonances. These types of faults determines overheating, ball bearings aging and operation of the machine at critical speeds (see equations 4-6). The current spectrum analysis highlights the presence of the side bands $\pm$ FL and $\pm$ 3 FL, around the rotation frequency of the rotor slots which does not correspond to the rotation frequency RS (Fig. 6 c).

- Misalignment between the electric motor and the coupling device determines the presence in the current spectrum of the frequency 1X, different from the rotation frequency (Fig. 6 d).

4 Applications and Experimental Results.

In the present section are presented two applications of the vibration signature method in determining faults on electrical machines.

Measurements must be properly performed, using an accurate system (accelerometers – vibration analyzer), in order that vibration amplitude vs. time and vs. frequency characteristics reflect the actual operation of the electrical machine.

The accelerometer is the primary device used in vibrations monitoring, representing a transducer which converts the acceleration generated by static and dynamic forces in electrical signals. It offers a large voltage excursion, covering the maximum vibration level, usually presenting a sensitivity of 1000 mV/g. Its sensitivity and frequency range are decisive for the selection. In case of electrical machines monitoring 10,000 Hz frequency range accelerometers should be selected.

A very important issue is to comply with standards from the point of view of mounting.

Accelerometers are connected to vibration analyzers, which can be set to measure vibration amplitudes, velocities and accelerations, along with the analysis versus time or frequency.

In the following applications, mono-channel [26] and three-channel [27] accelerometers were used, conceived for 3D determinations in a three-axis orthogonal system and adapted for three mono-axial accelerometers, placed coplanar on the electrical machine stator.

A first application (Fig. 7) refers to a production line for secure glass [28], where the monitoring system detected an overcome of the levels of the vibration velocity admitted by the standards.

Vibration measurements must be performed in compliance with ISO 10816 Standard [22], which provides vibration amplitude acceptance guidelines for rotating machinery operating from 600 until 12000 rpm, applied to electric generators, gas or steam turbines, turbo-compressors and vertical, horizontal or inclined shaft fans.

ISO 10816 Standard specifies the RMS vibration velocity limits on a basis of machine horsepower, and covers a frequency range from 10 Hz to 1,000 Hz. The limits in the standard are set in RMS values.

As measuring points, the ISO 10816 Standard guidelines recommend:

- for vertical or inclined mounted machines, areas with maximum value of vibrations must be chosen;
- measurements must be performed on accessible parts of the machines;
- measurements outcomes must have a high level of accuracy, representing the main vibrations and not the local resonation ones.

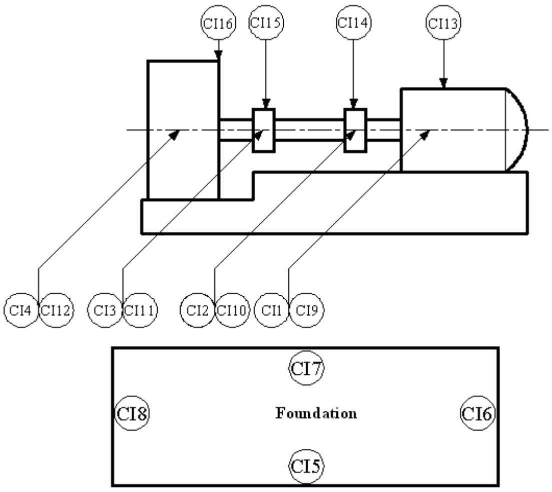

Fig. 7 The main measuring points

Table 1. Admissible vibration velocity limits according to ISO 10816 Standard.

Vibration Intensity	Foundation type	
v_{eff} [mm/s]	Qualification	
	Rigid Foundation	Elastic Foundation
0,46	good	good
0,71	good	good
1,12	good	good
1,8	good	good
2,8	satisfactory	good
4,6	satisfactory	satisfactory
7,1	admitted	satisfactory
11,2	admitted	admitted
18,0	not allowed	admitted
28,0	not allowed	not allowed
71,0	not allowed	not allowed

The ISO 10816 Standard Operation defines also the measurements conditions:

- measurements should be performed only in the steady state regime of rotor operation for constant speed and constant load drives;
- for adjustable speed drives (ASD), measurements must be performed in extreme conditions, covering the operation characteristics;

Moreover, ISO 10816 Standard, differentiates between rigid and elastic building foundations (Table 1), setting admissible vibration velocity limits.

The calculus of the RMS value of the vibration velocity using (equations 8-11) is rather complicated, especially if there are a lot of points in which the FFT (Fast Fourier Transform) must be considered.

A first set of measurements was carried out using mono-axial accelerometers in the case of the driving motor, in horizontal and vertical plane (Fig. 7).

Diagrams corresponding to the stator measuring points: acceleration vs. time (point C19, Fig. 8 a) and acceleration vs. frequency (point C19, Fig. 8 b) analyzed using the vibration signature method [25], could not identify the nature and the location of the fault, so a further examination became necessary.

The vibration acceleration in a plane perpendicular to the rotational axis, in three coplanar points displaced first at 120° and then at 90° respectively. Using equations (8)-(11), the velocity vector of for the two measurements setup can be determined (Fig. 9).

The main drawback of the method used in this application consisted in the use of mono-channel vibration analyzer [26], measurements in the three points being not simultaneous.

Following the recommendations of the European Directive 2002/44/EC [29], ISO 5349:2001 [30] and ISO 2631:1997 [31] Standards, vibration analyzers for tri-axial accelerometers were developed. These are especially dedicated to perform analyses of the vibrations transmission from building floors to humans.

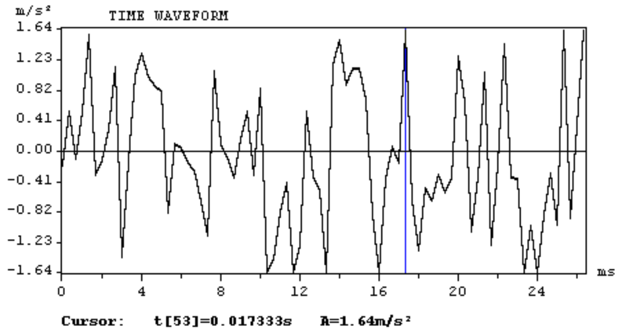

a- acceleration versus time

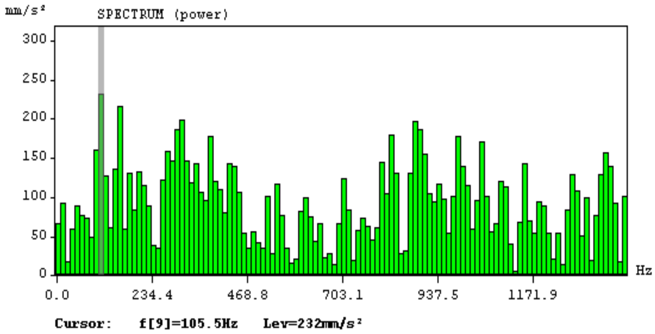

b- acceleration versus frequency

Fig. 8 Horizontal component of the vibration acceleration– point CI 19

Measurements were carried out using such an analyzer, namely SVAN 958 [27], and instead of the tri-axial accelerometer, three mono-axial accelerometers were mounted, in a plane perpendicular to the rotation axis of the electrical motor under diagnosis.

The fault direction on the electric motor's stator was determined, its value provides an indication concerning the faulty area: in the stator or in the rotor area of the electric motor.

The analysis vs. time and frequency of the measurements carried out using the software SVAN PC [32] eliminates the previous drawback, because it has the capacity of performing simultaneous measurements and calculus of the vibrations' directions in the three locations, making needless the use of the Equations (8)-(11).

The evaluation of the vibrations level is based on a vibrations level per hour A(1), expressed as a continuous equivalent vibration in one hour.

There is no need to perform measurements which overcome this duration, because in this time interval the vibration speed increases significantly. The data are normalized to one hour and the vibration level can be calculated using equation (14):

$$A(1) = v_{ae} \cdot \sqrt{\frac{T_e}{T_0}}, \tag{14}$$

where:

- v_{ae} represents the mean value of the weighted vibration speed during the measurements;
- T_e represents the total measurement interval;
- T_0 the time reference (one hour).

If the measurements are performed using three accelerometers (the analyzer SVAN 958 is designed for tri-axial accelerometers, so its connectors have been adapted for three mono-axial accelerometers), the total vibration speed of the electric motor under diagnosis being calculated using equation 15:

$$v_{ve} = \sqrt{v_{w1}^2 + v_{w2}^2 + v_{w3}^2} \tag{15}$$

the indices 1, 2 and 3 corresponding to the three accelerometers respectively.

The presented technique has been used in an application in which the vibration signature for two electric motors has been determined. The first was a faulty one (1.55 kW, 230 V/50 Hz, 1500 rpm), the second was a normal operating one (2.2 kW, 400 V/50 Hz, 2880 rpm). The two motors have been used in driving the pumps of the heating central in an office building [28].

5 Conclusions.

The vibrations signature analysis determined by the electric motors is quite a difficult task because in real situations the shape of the amplitude vs. frequency characteristics (see Fig 8b, 10b, and 11b) is much more complex than the shape of the ideal ones (see Fig. 1a to Fig.1 e), recommended in literature [25].

The experimental results of the first application highlights a vibration velocity vector determined using three accelerometers, mounted in two different positions on the stator periphery, which presents different magnitude and phase in the two situations depicted.

For a normal operation of a motor, the magnitude of the vector must be as lower as possible, having the same phase displacement or slightly different. However, for an accurate interpretation of the amplitude vs. frequency vibrations it is advisable to analyze also the amplitude-frequency characteristics of the stator current, in order to be convinced that current distortions or harmonics do not lead to extra-vibrations.

The result of the analysis obtained with mono-channel vibration analyzers presents the major drawback of the non-simultaneous measurements. The magnitude and the phase displacement between the two mounting positions (Fig. 9) highlights that the fault location is on the rotor, confirmed also by the comparison between the amplitude vs. frequency characteristics (see Fig. 1e and Fig. 8).

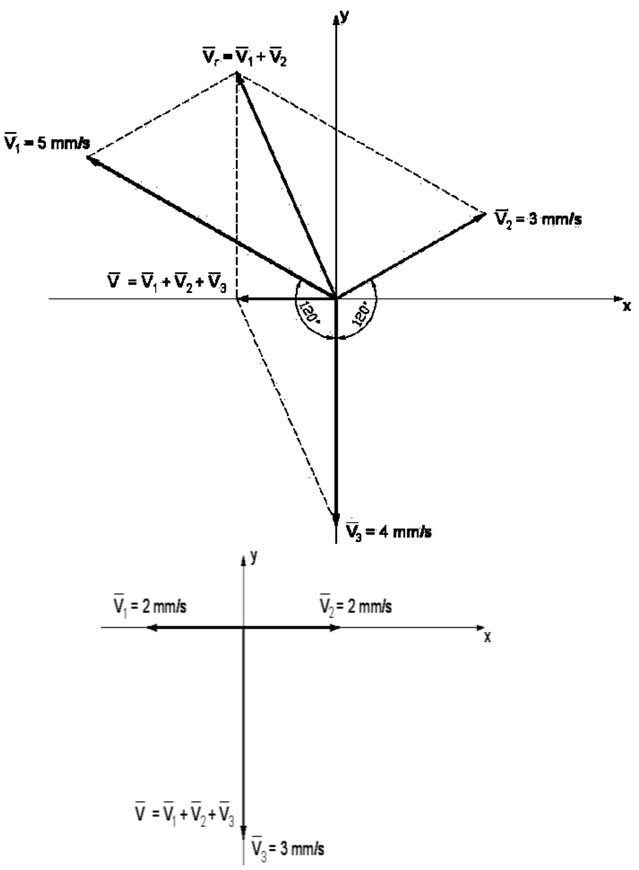

Fig. 9 The fault direction in the two measurement setups

The multi-channel analyzer used in the second application is more straightforward in measuring and interpretation of the measuring results. The amplitude vs. frequency characteristics in the case of the normal operating motor highlights that the fundamental component of the frequency is the power frequency (i.e. 50 Hz, in Fig. 10b), while for the faulty one is 1,000 Hz (Fig. 11b).

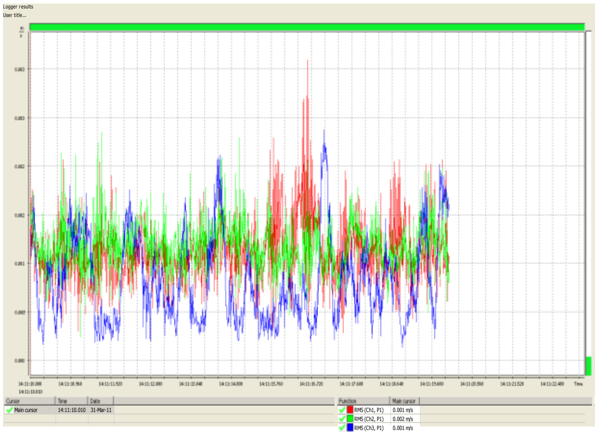

a-vibration vs. time signature

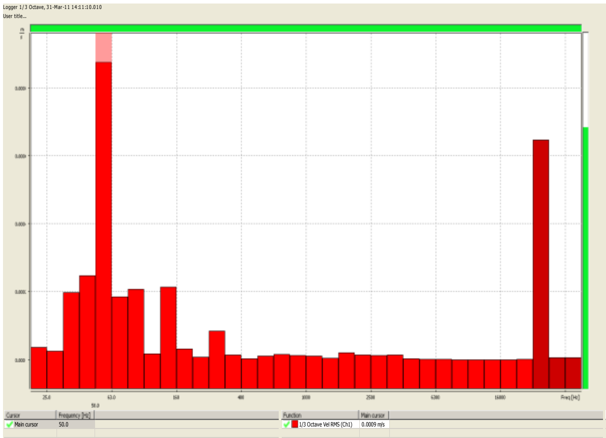

b-vibration vs. frequency signature

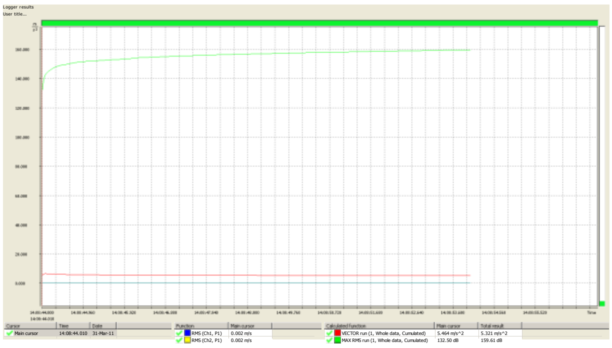

c-vector analysis

Fig. 10 The normal operating motor

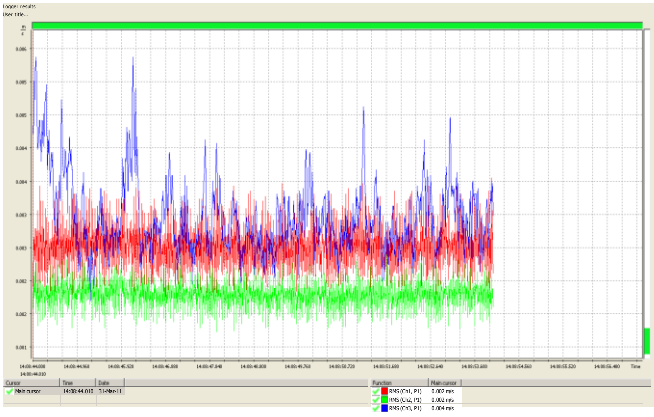

a-vibration vs. time signature

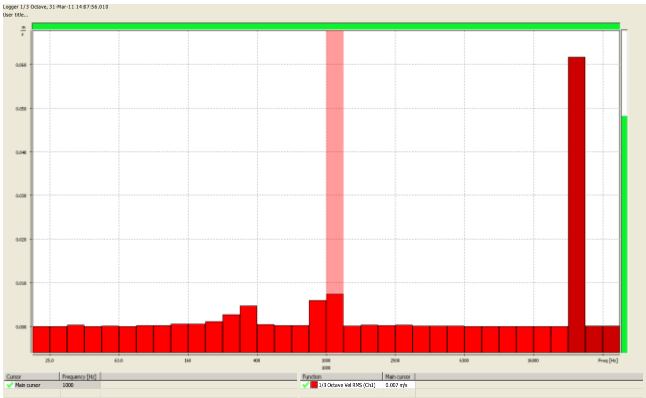

b-vibration vs. frequency signature

c-vector analysis

Fig. 11 The faulty motor

Another important advantage of the multi-channel analyzers consists in their software, which directly determines the vibration velocity vector, simultaneously for the three accelerometers and for the entire measurement duration.

For the normal operating motor, only a slight variation of the acceleration vector is recorded, its magnitude tending asymptotically to 160 m/s^2 (Fig. 11a).

For the faulty motor, the vibration velocity is changing permanently, from the minimum value of 250 m/s to the maximum one of 1,300 m/s.

As further work, the authors consider that a theoretical approach of the experiments depicted here is needed, along with the buildup of a data base, containing the direction diagrams corresponding to different faulty situations [33, 34].

6 References

Journal article

[1] M. R. W. Group, "Report of Large Motor Reliability Survey of Industrial and Commercial Installations, Part II," *IEEE Transactions on Industry Applications*, vol. IA-21, pp. 865-872, 1985.

[2] G. Bonnett, "Cause and analysis of stator and rotor failures in three-phase squirrel-cage induction motors," *IEEE Transactions on Industry Applications*, vol. 28, pp. 921-937, 1992.

[3] J. M. Grubic, B. Lu, T. G. Habetler, L. Salvatore, "A Survey on Testing and Monitoring Methods for Stator Insulation Systems of Low-Voltage Induction Machines Focusing on urn Insulation Problems,", *IEEE Transactions on Industrial Electronics*, vol. 55, p.p. 4127-4136, 2008.

[5] R. A. Kliman, J. Stein, R. D. Endicott, M.W. Madden, "Non-invasive detection of broken rotor bars in operating motors," *IEEE Transactions on Energy Conversion*, vol. 28, pp. 873-879, Dec. 1998.

[6] N. A. Mirafzal, "On innovative methods of induction motor interturn and broken-bar fault diagnostics," *IEEE Trans. Ind. Appl.*, vol. 42, pp. 405-414, Mar./Apr. 2006.

[7] Immovilli, F.,Bianchini, C., Cocconcelli, M.; Bellini, A.; Rubini, R., „Bearing Fault Model for Induction Motor with Externally Induced Vibration", IEEE Transactions on Industrial Electronics , Volume: PP, Issue: 99, 2012, ISSN : 0278-0046, DOI: 10.1109/TIE.2012.2213566.

[11] R. Wendell, "Using current signature analysis technology to reliably detect cage winding defects in squirrel-cage induction motors," *IEEE Transactions on Industry Applications*, vol. 43, p.p. 422-428, mar./apr. 2007.

[12] Henao, H.; Demian, C., Capolino, G., A frequency-domain detection of stator winding faults in induction machines using an external flux sensor, *IEEE Transactions on Industry Applications*, vol. 39, pp. 1272-1279, 2003.

[13] Gao, Z.; Colby, R. S.; Habetler, T. G. & Harley, R. G., A Model Reduction Perspective on Thermal Models for Induction Machine Overload Relays, *IEEE Transactions on Industrial Electronics*, vol. 55, no. 10, (October 2008) pp. 3525-3534, 2008.

[15] Kral, C.; Habetler, T. G. & Harley, R. G., Detection of Mechanical Imbalances of Induction Machines Without Spectral Analysis of Time-Domain Signals, *IEEE Transactions on Industry Applications*, vol. 40, no. 4, pp. 1101-1105, ISSN 0093-9994, 2004.

[16] J. A. Rajagopalan, J. M. Aller, T. G. Habetler, R. G. Harley, "Nonstationary Motor Fault Detection Using Recent Quadratic Time-Frequency Representations," *IEEE Trans. Ind. Appl*, vol. 44, pp. 735-744, 2008.
[17] H. Kia, G. A. Capolino, "A high-resolution frequencyestimation method for three-phase induction machine fault detection," *IEEE Trans. Ind. Electron.*, vol. 54, pp. 2305-2314,Aug. 2007.
[18] T. S. Khan, M. A. Rahman., "Real-Time Implementation of Wavelet Packet Transform-Based Diagnosis and Protection of Three-Phase Induction Motors," *IEEE Trans. Energy Conversion*, vol. 22, pp. 647-655, 2007.
[19] A. Ponci, L. Cristaldi, M. A. L. M. Lazzaroni, "Diagnostic of a Faulty Induction Motor Drive via Wavelet Decomposition," *IEEE Transactions on Instrumentation and Measurement*, vol. 56, p.p. 2606-2615, 2007.
[20] Leonard, F., Landry, C., Beauchemin, R., Turcotte, O., Brikci, F., "An Improved Algorithm Vibration Analysis as a Diagnostic Tool for Detecting Mechanical Anomalies on Power Circuit Breakers", *IEEE Transaction on Power Delivery*, vol. 23, no. 4, October 2008.
[21] M. Diallo, D. Hamad, X. Pierre, "Fault detection and diagnosis in an induction machine drive: A pattern recognition approach based on Concordia stator mean current vector," *IEEE Trans. Energy Convers.*, vol. 20, pp. 512-519, Sep. 2005.
[23] M. Boesing, T. Schoenen, K. A. Kasper, R. W. De Donker, "Vibration Synthesis for Electrical Machines Based on Force Response Superposition", *IEEE Transactions on Magnetics*, vol. 46, p.p. 2986-2989, Aug. 2010.
[33] Dorrell, D.G. "Sources and Characteristics of Unbalanced Magnetic Pull in Three-Phase Cage Induction Motors With Axial-Varying Rotor Eccentricity", *IEEE Transactions on Industry Applications*, Pages: 12 – 24, Volume: 47, Issue 1, 2011, DOI: 10.1109/TIA.2010.2090845.
[34] Concari, C., Franceschini, G., Tassoni, C., "Toward Practical Quantification of Induction Drive Mixed Eccentricity", *IEEE Transactions on Industry Applications*, Pages: 1232 – 1239, Volume: 47, Issue 3, 2011, DOI: 10.1109/TIA.2011.2124434.

Journal article only by DOI
[4] Kral, C.; Habetler, T. G.; Harley, R. G.; Pirker, F.; Pascoli, G.; Oberguggenberger, H. & Fenz, C. J.M. (2003). A Comparison of Rotor Fault Detection Techniques with Respect to the Assessment of Fault Severity, *Symposium on Diagnostics for Electric Machines, Power Electronics and Drives, SDEMPED 2003*, pp. 265-270, DOI: 10.1109/DEMPED.2003.1234584.
[8] Frosini L., Bassi E., Fazzi A., Gazzaniga C., "Use of the stator current for conditioning monitoring of bearings in induction motors", *Procc.of ICEM'08- XVIII International Conference on Electrical Machines*, Vilamoura (Algarve), Portugal,from 6th-9th September 2008, on CD, DOI: 10.1109/ICELMACH.2008.4799991.
[10] S. Nandi and H.A. Toliyat, "Condition Monitoring and Fault Diagnosis of Electrical Machines-A Review," *IEEE Ind. Appl. Society Annual Meeting*, 1999, DOI: 10.1109/IAS.1999.799956.
[14] Gaylard, A.; Meyer, A. & Landy, C., Acoustic evaluation of faults in electrical machines, *Seventh International Conference on Electrical Machines and Drives, IEE (Conf. Publ. No. 412), pp*. 147-150, 1995, DOI: 10.1049/cp:19950852.

Book
[9] P. Vas, "Parameter Estimation, Condition Monitoring, and Diagnosis of Electrical Machines," *Clarendon Press*, Oxford, 1993.

Online document (no DOI available)

[22] ISO 10816 “Mechanical vibration — Evaluation of machine vibration by measurements on non-rotating parts —Part 3: Industrial machines with nominal power above 15 kW and nominal speeds between 120 rot/min and 15 000 rot/min when measured in situ”, www.pruftechnik.com › Condition Monitoring.

[24] H. Balan, I.Vadan, S. Stefanescu, P. Karaisas, Vibro-Acoustic Diagnosis of a Ventilator Driving System, *Proceedings of the 2008 International Conference on Electrical Machines*, Paper ID 1081**;** Procc. of ICEM'08- XVIII International Conference on Electrical Machines, Vilamoura (Algarve), Portugal, 6th-9th September 2008, on CD, http://www.apdee.org/conferences/icem08.

[25] Frédéric Champavier, “Condition Monitoring of Induction motors using Vibration and Electrical signature analysis*,” EE Mods Conference14-17 september 2009*, Nantes, France, www.docstoc.com/.../Condition-Monitoring-of-Induction-Motors-Usi...

[26] *** SVANTEK „SVAN 912 AE Four Channels Sound & Vibration Analyzer” Technical Book, www.svantek.com.

[27] *** “Noise and vibration analyzer SVAN 958”, Technical Book, www.svantek.com.

[28] Vibro-acoustic diagnosis for ventilators driving system of UNIGLASS equipment type UGT-2400x4200. Contract 35/2007, www.utcluj.ro.

[29] *** “Directive 2002/44/EC for occupational vibration exposure”, www.ueanet.com/facts2/summ/sum-02-44-en.pdf.

[30] *** ISO 5349:2001 “Measurement and evaluation of human exposure to hand-transmitted vibration”, www.freestd.us › Standards Worldwide.

[31] *** ISO 8041:2005 “Human Response to Vibration – Measuring Instrumentation”, www.iso.org/iso/catalogue.

[32] Svan PC Software, www.svantek.com.